RESEARCH

Linkage mapping and genome annotation give novel insights into gene family expansions and regional recombination rate variation in the painted lady *(Vanessa cardui)* butterfly

Daria Shipilina*[,1,2*], Karin Näsvall*[,1], Lars Höök[1], Roger Vila[3], Gerard Talavera[4] and Niclas Backström[1]

Abstract

Gene family expansions and crossing over are two main mechanisms for the generation of novel genetic variants that can be picked up by natural selection. Here, we developed a high-density, pedigree-based linkage map of the painted lady butterfly (*Vanessa cardui*) - a species famous for long-distance migratory behavior, lack of diapause and extreme polyphagy. We also performed detailed annotations of genes and interspersed repetitive elements for a previously developed genome assembly, characterized species-specific gene family expansions and the relationship between recombination rate variation and genomic features. Identified expanded gene families consisted of clusters of tandem duplications with functions associated with protein and fat metabolism, detoxification, and defense against infection - key functions for the painted lady's unique lifestyle. The detailed assessment of recombination rate variation demonstrated a negative association between recombination rate and chromosome size. Moreover, the recombination landscape along the holocentric chromosomes was bimodal. The regional recombination rate was positively associated with the proportion of short interspersed elements (SINEs), but not the other repeat classes, likely a consequence of SINEs hijacking the recombination machinery for proliferation. The detailed genetic map developed here will contribute to the understanding of the mechanisms and evolutionary consequences of recombination rate variation in Lepidoptera in general. We conclude that the structure of the painted lady genome has been shaped by a complex interplay between recombination, gene duplications and TE-activity and that specific gene family expansions have been key for the evolution of long-distance migration and the ability to utilize a wide range of host plants.

Keywords: genomics; recombination; linkage map; gene family

Introduction

The genomics era opens up opportunities for investigating relationships between genotypes and complex phenotypes on a novel level and a better understanding of genome evolution. Combinations of different approaches can lead to novel insights into the dynamics of recurring duplications, deletions and other types of structural rearrangements, for example, by assessing molecular mechanisms and evolutionary consequences of gene family expansions and contractions, the activity of selfish genetic elements (e.g. transposable elements, TEs) and recombination rate variation.

Gene duplication has since long been recognised as an important mechanism for generating novel genetic material for natural selection to act upon [1, 2, 3], and gene family expansions and contractions are important sources for generation of phenotypic diversity [4, 5]. Comparative approaches, such as orthology analysis, allow for identification of expanding or contracting gene families and annotation of specific orthogroups (i.e. gene sets originating from a single gene copy in the common ancestor of the focal taxa) can aid in the assessment of the functional relevance of gene copy number variation in the evolution of lineage-specific traits. This approach might be beneficial for investigating complex phenotypes, where combined effects of different types of genetic changes likely underlie the trait [6]. Comparative analysis of gene expansion can complement traditional comparative studies of sequence changes in single orthologous genes, especially when comparing more distant taxa.

Since the spearheading work by McClintock [7], transposable elements (TEs) have been acknowledged as major contributors to different types of evolutionary change in eukaryotes [8, 9]. Transposable elements are

*Correspondence: daria.shipilina@ebc.uu.se
[1]Department of Ecology and Genetics, Uppsala University, Norbyvägen 18D, 75236 Uppsala, Sweden
[2] Swedish Collegium for Advanced Study, Thunbergsvägen 2, 75236, Uppsala, Sweden
Full list of author information is available at the end of the article

capable of self-replication within the host genome, resulting in the presence of multiple interspersed copies, which in turn can mediate both small scale deletions and duplications and large scale chromosome rearrangements [9]. In addition, TE insertions can affect gene function when regulatory or coding regions are targeted. Although this can sometimes lead to an instant selective advantage [10], TE propagations predominantly have neutral or deleterious effects on the host [11]. The proliferation of TEs in the genome of a host organism can be considered a selfish process since TEs enhance their transmission, a process that leads to the rapid diversification of many eukaryotic genomes [12]. In Heliconius butterflies, TE diversification has likely contributed to the formation of reproductive barriers [13], and in other butterfly lineages, rapid accumulation of TEs has resulted in considerable genome size expansions [14, 15]. Therefore, characterisation of the TE repertoire is key to understanding the microevolutionary dynamics within the genome of a species and the potential effects of TE activity on trait variation within populations and between species.

Besides gene duplication and TE activity, recombination is a process crucial for evolutionary innovation. Meiotic recombination shuffles existing segregating genetic variants, resulting in the generation of novel haplotypes [16]. Recombination also influences selection efficiency by directly preventing the accumulation of deleterious alleles (Müller's ratchet) and breaking the physical linkage between mutations with different selective effects (Hill-Robertson effects). The rate of recombination can vary on different scales. Of particular interest for population genetic processes is the variation in recombination rate between different genomic regions. Such spatial variation in the recombination rate has been observed in many different organisms [17, 18]. However, besides detailed recombination maps in the butterfly genus Heliconius [19], little is known about how the rate of recombination rate varies across chromosome regions in Lepidoptera and how recombination is associated with different genomic features [20, 21].

As indicated above, incorporating different approaches is essential for studying the genetic underpinnings of complex phenotypes and the mechanisms governing microevolutionary processes. The painted lady, Vanessa cardui, represents a key study system for a wide array of evolutionary studies. It is the most cosmopolitan of all butterfly species [22], and its migratory behavior includes a diverse repertoire of distinct phenotypes. In general, strictly migratory butterfly species need to sustain long-distance flight and have well developed navigational abilities [23]. Therefore, traits related to energy metabolism, sensory reception and the flight machinery likely have been under strong directional selection. In contrast to many other migratory butterfly species, painted lady is a non-diapausing, multigenerational migrant, with an annual migratory circuit covering areas with extreme environmental heterogeneity [24]. Despite the high risks associated with such a migratory lifestyle, painted ladies have successfully colonized almost all continents, and the species harbors high levels of genetic diversity, indicating a large effective population size [25]. This is, at least partly, probably a consequence of the species' ability to utilize an unusually wide range of host plants [26, 23]. Until the era of high-throughput sequencing, the possibilities to gain insights into how the migratory and generalist lifestyle has been manifested at the level of the genome have been limited: genetic basis of migratory behavior only has been investigated in a few model species (e.g. the monarch butterfly) so far [27].

A key step for genomic analyses is the development of a high-contiguity genome assembly of the focal species together with a thorough genome annotation. A powerful method to generate a chromosome level physical assembly and ensure its spatial correctness is a construction of a linkage map. In this study, we present the first detailed linkage map of the painted lady and verify scaffolds from a previously available genome assembly based on long-read sequencing technology (Darwin Tree of Life project [DToL]). We use the genome annotation and linkage information to quantify lineage-specific patterns of gene family evolution, relative TE abundance and how the regional recombination rate variation is associated with genomic features in the painted lady. Our analyzes complement earlier efforts to establish genomic tools for this species [28, 29] and give novel insights into the overall genome structure, recombination rate variation and lineage-specific gene family expansions in this species, information that informs on the molecular mechanisms underlying genome evolution in butterflies in general and the formation of the complex migratory phenotype and extreme generalist lifestyle of the painted lady in particular.

Results

Linkage map and genome annotation

To verify the chromosome level assembly and to get access to detailed recombination rate data, we constructed a pedigree-based linkage map. The total distance of the linkage map was 1,516 centiMorgan (cM) and contained 1,323 markers. When anchored on the 424 Mb physical assembly, the average marker density was 3.09 markers / Mb. The genome assembly was highly collinear with the marker order in the linkage map (Pearson's correlation coefficient; $R = 0.91$-1.00, p-value $> 1.00 \times 10^{-04}$, Figure S1) and consisted

of 30 autosomes and the sex chromosomes Z and W. The high collinearity between linkage groups and assembled scaffolds, the large scaffold N50 (14.6 Mb) and high BUSCO scores (97% complete arthropod genes) confirm that the scaffolds in the assembly essentially represent complete chromosomes that could be used for accurate characterization of genomic features and quantification of regional recombination rate estimates.

In total, TEs constituted > 150 Mb (37.40%) of the assembly and LINEs and SINE were the most abundant of the repeat classes that could be categorized (Table 1). After automatic annotation and subsequent manual curation, 13,161 protein-coding genes were identified (including 89.90% BUSCO genes), of which 12,209 had functional annotation information (Table 1). Visual inspection of the spatial distribution of genes and TEs along chromosomes revealed rather similar distributions of repeat classes between autosomes and the Z-chromosome, but also an observable excess of repeats on smaller autosomes and a striking difference in repeat composition and gene density on the W-chromosome (Figure 1).

Table 1 Linkage map, genome assembly and annotation statistics

Linkage map	
Total map length (cM)	1,516
Number of markers	1,323
Markers per physical distance (N / Mb)	3.09
Genome assembly	
Scaffold N50 (bp)	14,615,999
GC content	33.41%
Total repeat proportion	37.40%
Repeat content (% of total repeat proportion)	
SINEs	7.30%
LINEs	14.94%
LTR elements	2.47%
DNA elements	3.04%
Simple and unknown repeats	30.17%
Gene annotation	
BUSCO genes (complete arthropoda)	89.90%
Number of protein coding genes	13,161
Number of genes with functional annotation	12,209

Synteny

The level of large-scale structural conservation of the painted lady genome was assessed by comparing gene order on the painted lady chromosomes to two previously available high-contiguity lepidopteran genome assemblies positioned at different levels of divergence in the lepidopteran tree of life, the silkmoth (*Bombyx mori*) and the postman butterfly (*Heliconius melpomene*). Overall the synteny was highly conserved between the painted lady and the other species, but chromosomes 28 and 26 mapped to the same chromosome (24) in *B. mori* and the previously described fusions of several chromosomes in the *H. melpomene* genome [30] could also be verified (Figure 2). In summary, this confirms that the painted lady karyotype is highly similar to the inferred ancestral butterfly karyotype [31].

Gene family evolution

To investigate the turnover of specific gene families in the painted lady, we analyzed a set of nine representative nymphalid species with detailed annotation information (see methods). The non-migratory *Vanessa tameamea* was included to assess differences in gene family evolution between sedentary and migratory lineages within the Vanessa genus. We found that 93.2% (1,288,332) of the total number of genes from the nine nymphalid species were clustered in 14,027 orthogroups. The percentage of genes assigned to orthogroups varied from 86.7 to 99.6% in the different species (Table S1). In the painted lady, 96.4% (12,692) of the annotated genes were assigned to 10,361 orthogroups with 19 lineage-specific orthogroups containing 63 genes (Table S1). Within the Vanessa genus, 65 expansions have occurred on the ancestral Vanessa branch, 648 on the *V. cardui* branch and 1,563 on the *V. tameamea* branch.

We used a maximum likelihood model to detect genes with distinct gene family expansion rates in the painted lady compared to the other species. The analysis showed that 15 orthogroups were significantly expanded in the painted lady. The orthogroups contained 77 genes, of which 34 had associated GO-terms (Figure 3). Among the largest expanded gene families were two classes of proteases, a lipoprotein receptor and the Lepidoptera-specific moricin immune-gene family. Analysis of the spatial distribution of extended orthogroups revealed clustering/tandem duplications for all except one of the orthogroups (Figure 3C). Significantly enriched GO-terms for expanded gene families in the painted lady were predominantly associated with protein degradation, muscle function and development, and fatty acid and energy metabolism (Figure 3A). Multiple ontology terms were shared between expanded orthogroups, pointing towards similar functions associated with the different gene families (Figure 3B). To assess potential convergence between migratory species, we also identified gene families with a distinct gene expansion rate in the two migratory lineages (the painted lady and the Monarch butterfly, *Danaus plexippus*), compared to the other nymphalids. This analysis revealed 11 orthogroups with a higher expansion rate and 29 orthogroups with genes specific to these two species. The common orthogroups

Figure 1 Distribution of repeat classes and genes as estimated along the painted lady chromosomes (100 kb windows). Density (% of the window covered) of different TE classes are illustrated with distinct colors cumulatively added on top of each other above the X-axis and density of genes below the X-axis (legend to the top right).

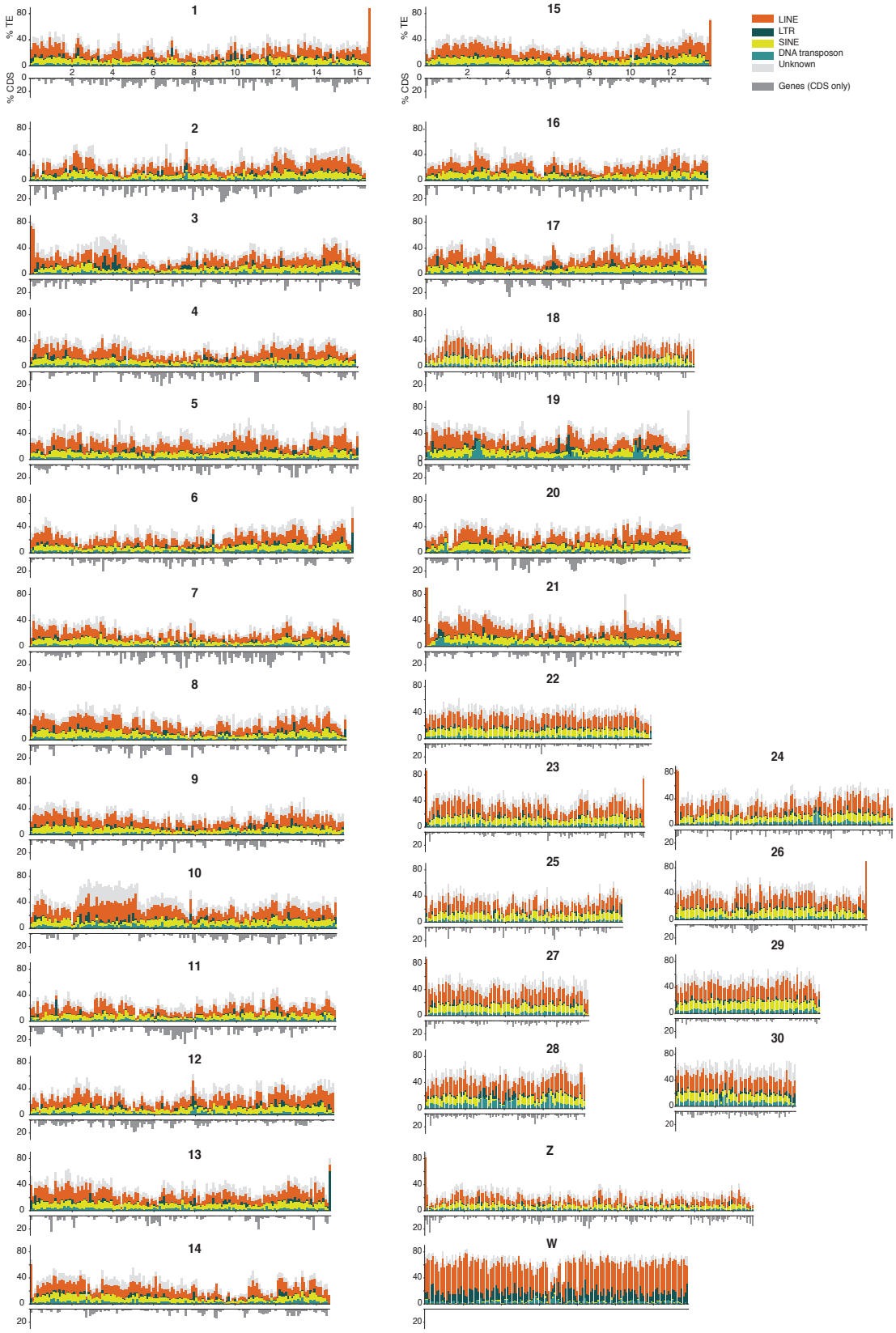

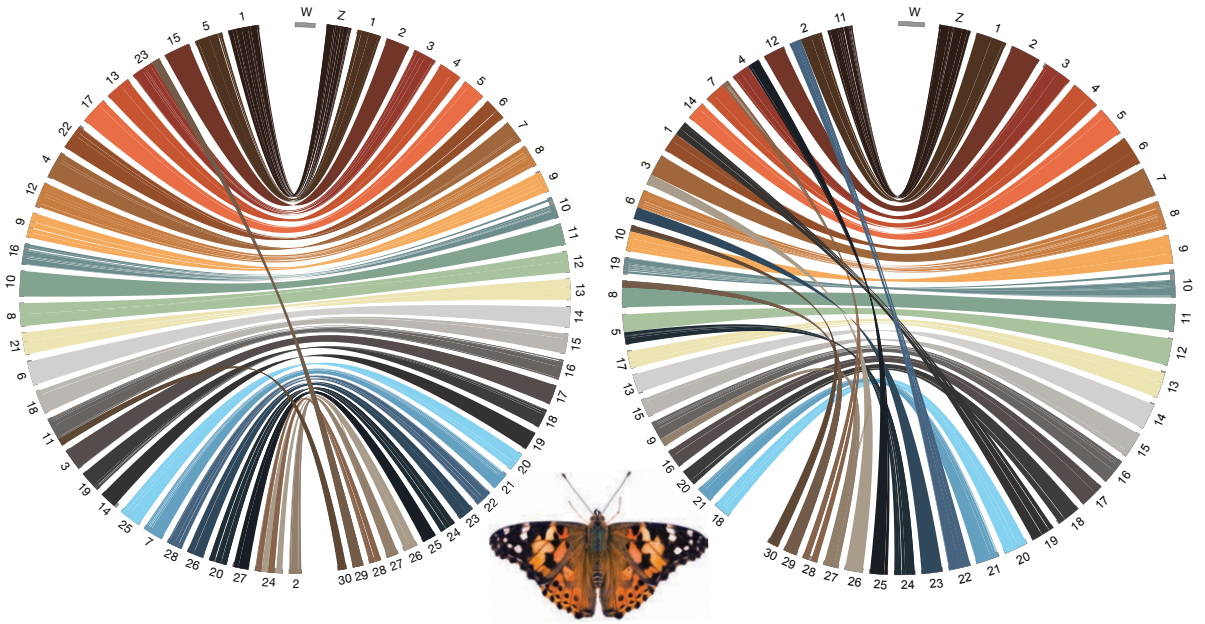

Figure 2 Synteny between the painted lady and a) the silkmoth and b) the postman butterfly chromosomes, respectively. The painted lady autosomes are sorted and named according to length and the sex chromosomes are indicated with Z and W. Orthologous genes are connected with lines. Colors represent individual chromosomes.

included 112 genes and were significantly enriched for GO-terms predominantly associated with metabolic processes, defence against infection and neuronal activity (Figure S2).

Patterns of recombination rate variation

Global and chromosome specific recombination rates

The development of a detailed linkage map allowed both for estimating the global recombination rate in the painted lady and to investigate potential regional recombination rate variation and association with genomic features. The average, genome-wide recombination rate was 3.81 cM / Mb (W-chromosome excluded), but there was considerable inter-chromosomal variation (2.21 - 8.00 cM / Mb; Table S2, Figure S3), with a significantly higher rate on shorter chromosomes than on longer chromosomes (Figure 4). The recombination rate on the Z-chromosome was 3.09 cM / Mb, lower than the average unweighted autosomal rate. However, the recombination rate on the Z-chromosome was not lower than expected given the overall negative correlation between recombination rate and chromosome size (Spearman's rank correlation, $p = $-0.83, p-value $= 6.51\times10^{-07}$; (Figure 4A). Besides the negative association between chromosome size and recombination rate, we also found significant negative associations between chromosome size and GC-content ($p = $-0.65, p-value $= 8.35\times10^{-05}$) and repeat density ($p = 0.77$, p-value $= 1.37\times10^{-06}$), and a positive association with gene density ($p = .68$, p-value $= 2.63\times10^{-05}$)(Figure 4B,C,D).

Intra-chromosomal variation in recombination rate and associations with genomic elements

To quantify potential regional variation in recombination rate within chromosomes, we estimated the recombination rate in 2 Mb non-overlapping windows along each individual chromosome. The average rate across windows was similar to both the global rate estimate across chromosomes (4.05 +/- 2.45 cM / Mb) and the overall chromosome level estimates (2.58 - 7.53 cM / Mb, W-chromosome excluded). The recombination rate estimates for individual windows ranged between 0 - 14.79 cM / Mb (Figure S3, Table S2) and visual inspection revealed a bi-modal distribution with reduced recombination rate in the center of chromosomes and towards chromosome ends (Figure 4 E-H). To test this observation formally, we analyzed the difference in recombination rate between bins representing five relative distance intervals from the center of the chromosome for all chromosomes combined and found that the recombination rate was significantly lower in the center (first bin), significantly higher in the flanking terminal (fourth) regions and then again lower at the terminal end (Wilcoxon rank sum test, p-value $< 3.70\times10^{-02}$ - 6.30×10^{-15}, Figure S4).

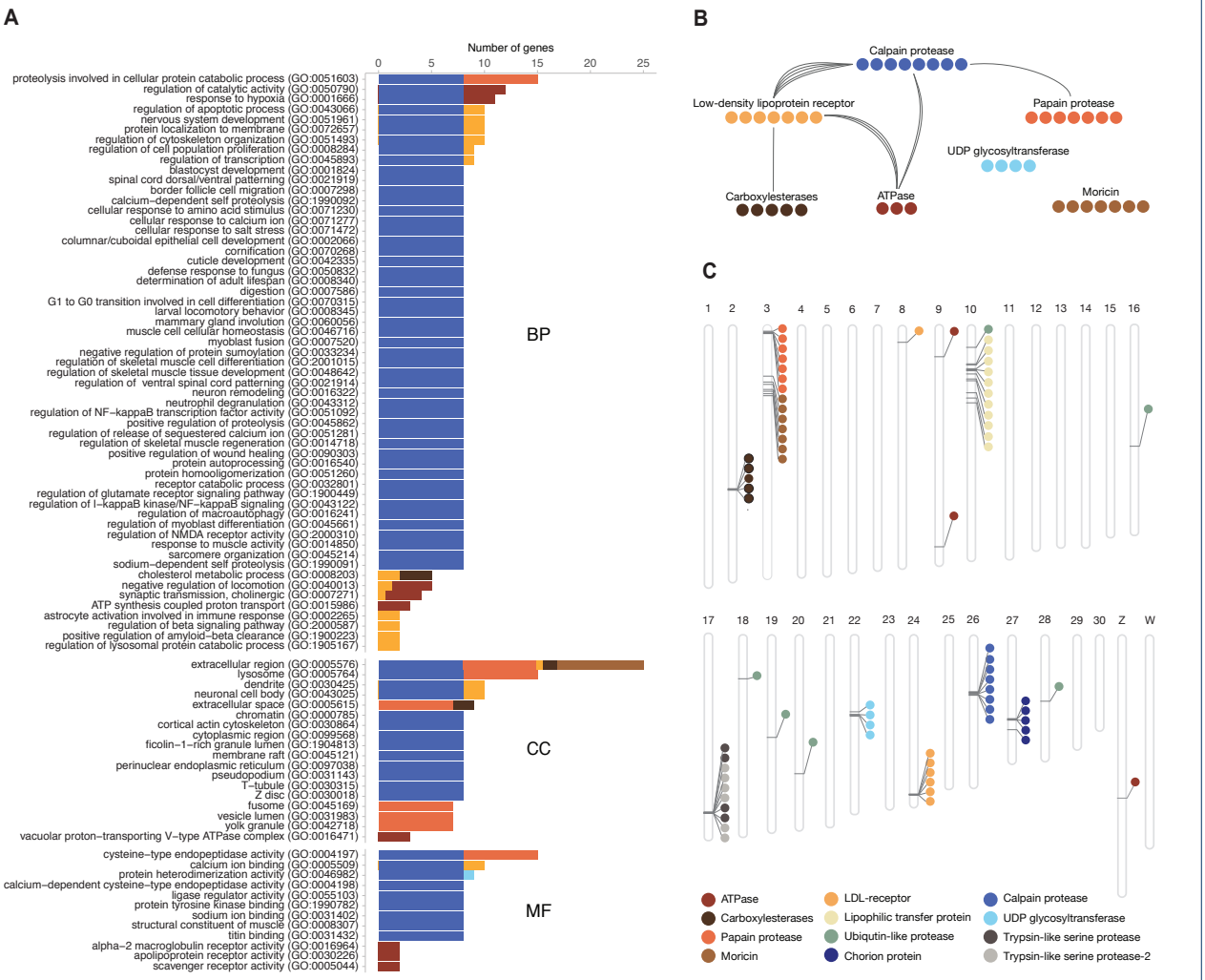

Figure 3 A) Significantly (p-value < 0.05 after FDR-correction) enriched gene ontology (GO) terms associated with expanded gene families in the painted lady. The bars show the number of genes associated with each GO-term. The different GO-categories are biological process (BP), cellular compartment (CC) and molecular function (MF). B) Orthogroups with significantly enriched GO-terms. Shared GO terms between ontology terms (biological process category only) are shown in connecting lines. C) Spatial distribution of genes from extended orthogroups identified in BadiRate analysis.

To assess potential relationships between the recombination rate and genomic features in more detail, we first investigated different associations between the window-based recombination rate estimates and variation in nucleotide composition and proportions of different TEs and genes. The W-chromosome was excluded from this analysis since it is non-recombining in Lepidoptera. We found that the GC-content increased towards the ends of chromosomes and was positively associated to the regional recombination rate ($p = 0.32$, p-value $= 3.68 \times 10^{-06}$). Gene density was homogeneous across chromosomes, with only a minor increase towards the chromosome center, and was negatively associated with the recombination rate ($r = -0.19$, p-value $= 7.27 \times 10^{-03}$). We found a significant positive association between the overall repeat proportion and the recombination rate (p= 0.35, p-value = 3.48e-07; Figure 5), and this pattern was consistent for all repeat classes, but strongest for SINEs ($p = 0.42$, p-value $= 2.63e^{-10}$) and weakest for LTRs ($p = 0.14$, p-value $= 4.04e^{-02}$). The association between recombination rate and proportion of LTRs was, however, not significant when only including autosomes ($p = 0.11$, p-value $= 11.04e^{-02}$) (Figure 5, Figure S5).

To disentangle the relative strength of associations between the regional recombination rate and genomic features, a multiple linear model was implemented with recombination rate as the dependent variable.

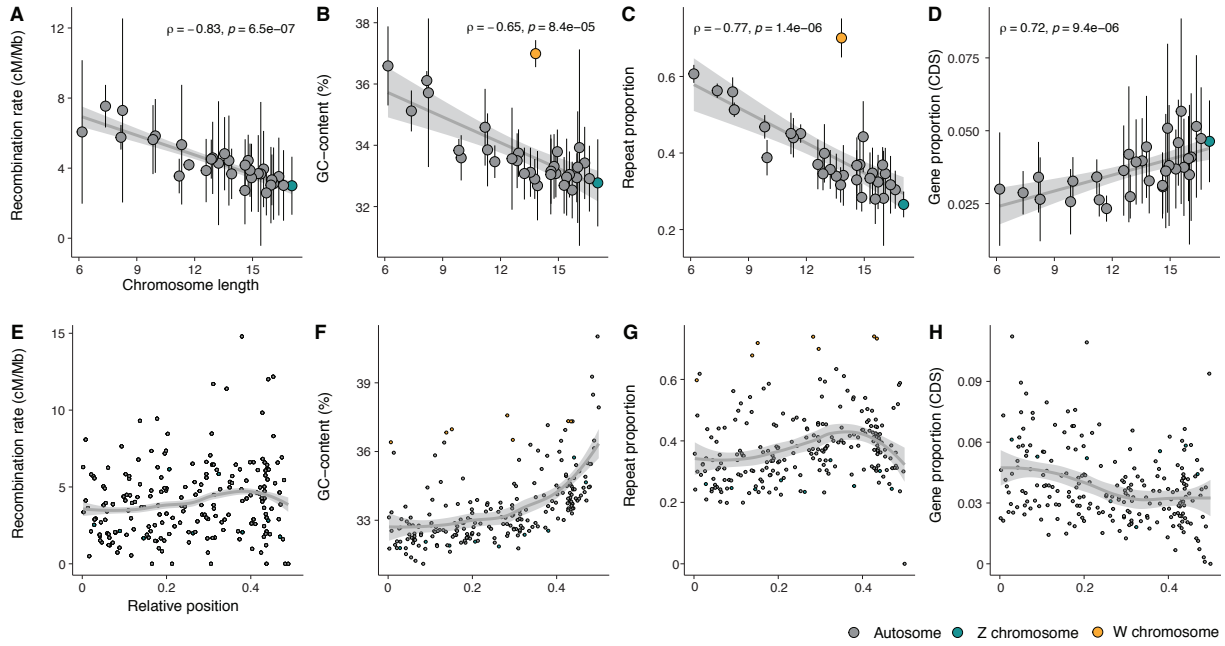

Figure 4 Top row: Associations between chromosome length and A) recombination rate, B) base composition, C) repeat content and D) gene density. Chromosome length is given in megabases (Mb). Bottom row: Regional distribution of the recombination rate (E), base composition (F), repeat density and gene density in 2 Mb windows along the chromosomes. All chromosomes were analyzed jointly and the y-axis shows the relative position (proportion of chromosomal length) from the center of the chromosomes.

As explanatory variables we used chromosome length, chromosome type, GC-content, proportion of genes (CDS) and proportions of all different classes of TEs. We found that the regression model was significant ($df = 197$, $F = 7.73$, p-value $= 5.36\times10^{-09}$) and explanatory variables in the model accounted for 21% of the variation in recombination rate ($R2 = 0.24$, $adjR2 = 0.21$). Most of the variation was explained by the positive association with the proportion of SINEs (est 1.59, p-value $= 9.75\times10^{-04}$) and the negative association with chromosome size (est -0.48, p-value $= 4.88\times10^{-02}$; Figure 5, Table S3).

Finally we explored whether gene expansions could be associated with other genomic features, and we therefore compared TE abundance in the regions with and without gene gains. The mean densities of LTRs, LINEs and DNA transposons were higher in regions with gene gains (Wilcoxon rank sum test, p-value 3.1×10^{-03} - 6.0×10^{-04}, Figure S6), as was mean GC-content (p-value 3.0×10^{-02}). The gene densities or recombination rates did not differ between regions with and regions without gene gains (Wilcoxon rank sum test, p-value, 9.1×10^{-01} and $8.\times10^{-01}$, Figure S6).

Discussion

General

Here we present detailed results on the genomic architecture and regional recombination rate variation in the painted lady. The data paves the way for understanding the interplay between molecular mechanisms and micro-evolutionary processes shaping the genome of butterflies in general and provide the first insights into the links between genomic features and the unique lifestyle of this species. The rapid technological advances and dropping costs of DNA-sequencing methods have led to a staggering development rate of high-quality genome assemblies, including many butterfly species [32, 33, 34, 35, 36], and the availability of genomic resources will probably increase almost exponentially in the near future, as a result of the Darwin tree of Life (/https://www.darwintreeoflife.org/), the European Reference Genome Atlas (ERGA; https://www.ergabiodiversity.eu/) and other similar initiatives. However, detailed and curated genome annotation data are more time-consuming and expensive to generate and therefore still limiting comparative/population genomic and genotype-phenotype association approaches, not the least in butterflies [30, 37, 38]. Another limiting factor for understanding both genome architecture in general, the relative effects of random and selective

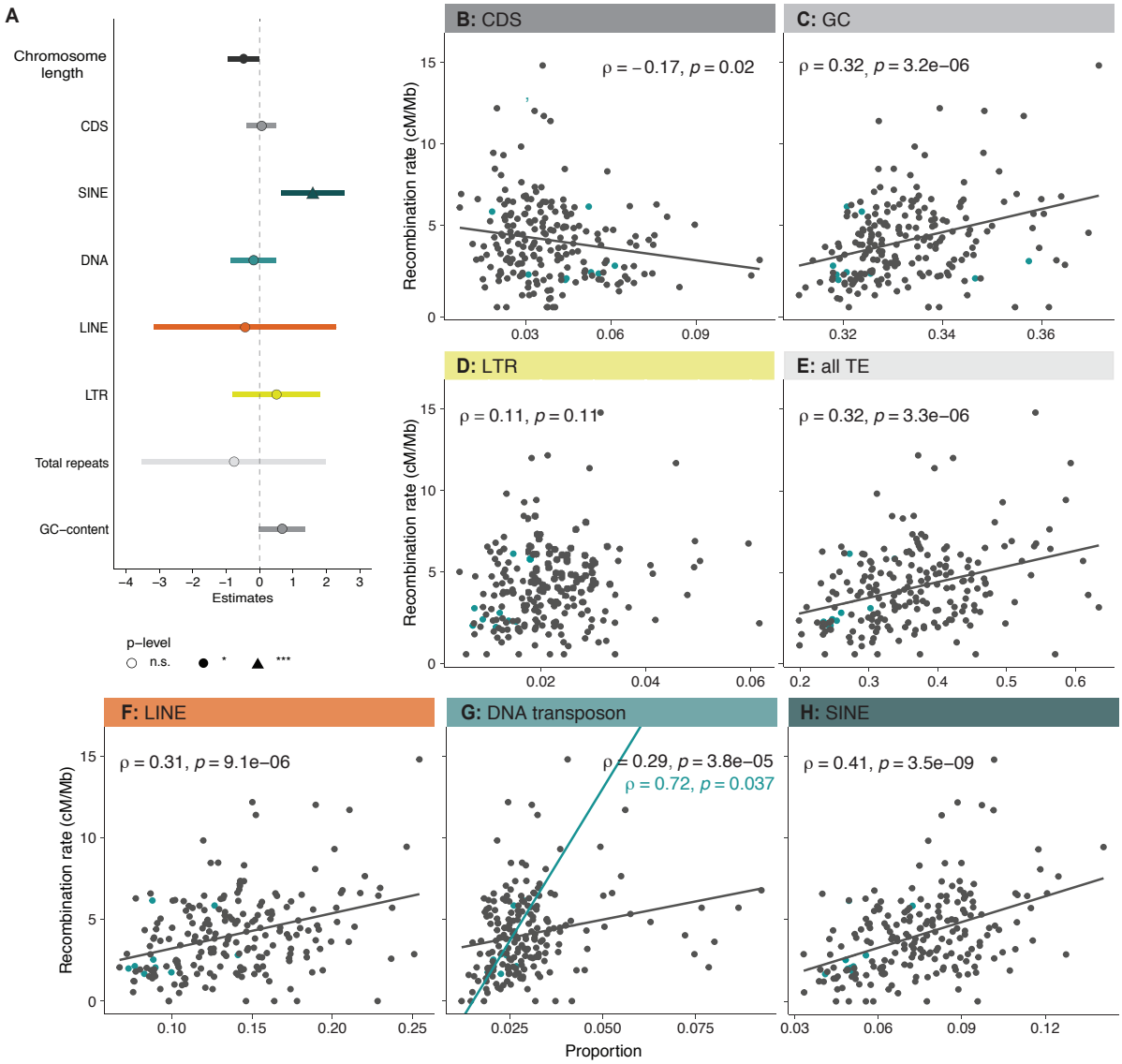

Figure 5 Correlation between recombination rate and density of genomic features. A) Summary of the linear model with regional recombination rate as the response variable. Each explanatory variable in the model is listed along the Y-axis and the relative estimated effect (X-axis), and error intervals are indicated with horizontal bars for each variable. B - H) Associations between the regional recombination rate and specific genomic features. Linear regression lines, Spearman's correlation coefficients (ρ) and the corresponding p-values for significant analyzes are given. Gray dots/lines indicate autosomal regions and turquoise dots/lines Z-chromosome linked regions

forces on sequence evolution and maintenance/loss of genetic diversity, and divergence processes, is that detailed recombination rate data are both laborious and time-intensive to gain, especially for natural populations. As a consequence, high-density recombination maps are still lacking for the vast majority of wild species where genome assemblies are now available. The detailed annotation information and the high-density linkage map for the painted lady developed here, therefore provide opportunities for both comparative studies on genome structure organization, population genomic- and micro-evolutionary investigations in the entire Lepidoptera clade.

Chromosome numbers have been shown to vary considerably between different butterfly and moth species; the haploid chromosome counts range from 5 to 223 [39, 40]. In agreement with previous data [29], both the linkage map and the DToL genome assembly clearly

showed that the painted lady has a total haploid chromosome count of 31. We confirmed high levels of synteny and gene order collinearity between the painted lady and the silkmoth, and the lineage specific chromosome fusions characterized before in the postman butterfly [30]. Hence, similar to other nymphalid butterflies, the painted lady has retained the inferred ancestral lepidopteran karyotype [31]. The annotation procedure revealed that the painted lady harbors a gene set (n = 13,161) close to the suggested core set in Lepidoptera [41, 42] and a relatively low overall TE content. However, the TE content was significantly higher and the gene density lower on smaller chromosomes. A clear outlier for gene density and TE content was the W-chromosome. While having a size equal to an average autosome, the W-chromosome demonstrated very specific features; both a significantly higher overall proportion of TEs, a larger fraction of longer TEs, and a different distribution of repeat classes compared to other chromosomes. Similar to the silkmoth and julia heliconian (*Dryas iulia*), the W-chromosome in the painted lady had a significantly higher proportion of LTRs and LINEs [43, 44]. The proportion of SINEs was however much smaller on the W-chromosome than on the autosomes and the Z-chromosome. A lack of protein coding genes, like we observed on the the painted lady W-chromosome, has also been observed in the silkmoth [45, 44], and is likely a consequence of the general degradation process of the non-recombining sex-chromosome [46]. The higher accumulation of TEs is also an expected consequence of recombination suppression and comparatively low effective population size (N_e) of the W-chromosome (1/4 of the autosomes at equal sex-ratios), both as a consequence of Müllers ratchet and since the overall efficiency of selection against TE insertion is reduced for non-recombining chromosomes [46]. The Z-chromosome is generally highly conserved in Lepidoptera [47] and it is the largest of all the painted lady's chromosomes. We did not find any significant differences in gene or TE content on the Z-chromosome compared to the autosomes.

Gene family analysis

Gene family expansions can provide the raw material for both neo- and sub-functionalizing evolutionary directions, and the rate of gene duplication can be significantly higher than the rate of function-altering single nucleotide mutations [48]. However, most gene duplication events are probably deleterious [49] or effectively neutral, leading to a low probability of fixation of novel gene copies [50]. We found a comparatively low proportion of lineage-specific gene duplications in the painted lady, which could be a consequence of the large Ne of the species, which translates to efficient selection against slightly deleterious variants. The majority of the (comparatively few) significant gene expansions in the painted lady clustered on single chromosomes - only a single gene family had expanded and dispersed across multiple chromosomes - suggesting that unequal crossing over has been the main mechanism behind gene family expansions in the species.

Vanessa cardui has extraordinary life-history characteristics and has become a quickly uprising complementary model organism for studying insect migration. Over most of the nearly cosmopolitan distribution range [51], the painted lady individuals annually complete a multigenerational migratory circuit that can span many thousand kilometers in total, and single individuals can migrate $> 4,000$ kilometers during lifetime [52, 24]. In addition, the painted lady is an extremely polyphagous generalist that utilizes > 300 different larval host-plants [26, 53, 54] and, in contrast to other migratory butterflies like the monarch and the red admiral (*Vanessa atalanta*), the painted lady is non-diapausing [51]. This unique combination of life-history traits is accompanied by high levels of heterozygosity and presumably a very large effective population size [25]. The genetic underpinnings of migratory behavior have only been preliminarily characterized for a handful of insect species [55, 56]. The genetic compositions underlying the lineage-specific adaptations in the painted lady have not been studied. The dissection of potential associations between genetic (and epigenetic) variants and complex phenotypes like 'migratory behavior' obviously requires a combination of multiple approaches. As the first step to understanding lineage-specific characteristics of the painted lady, we here focused on gene family evolution. Our results showed a limited number of genes with significant copy number expansions unique to the painted lady lineage. The expanded gene families were mainly associated with functions related to the transport of fatty acids, protein metabolism, and muscle structure/activity. Since insects mainly use fat as an energy resource during migration [57, 58, 59, 60], both the capacity to build up fat deposits and efficient sequestration of fatty acids have likely been under strong selection in the painted lady. Likewise, enhanced muscle structure and function should be advantageous for long-distance migrants compared to sedentary species. Therefore, efficient fine-tuning and optimization of fatty acid metabolism and increased muscle sustainability during migration could have been aided by the expansion of specific gene sets involved in those processes.

Besides the obvious advantages of having efficient energy metabolism and high-functioning flight machin-

ery, long-range migrants will also benefit from utilizing a multitude of different host plants since they will encounter dramatically different habitats, both during the lifespan of single migratory individuals and between consecutive generations. In contrast to the monophagous monarch butterfly, painted lady can utilize a wide range of host plant species [54], an adaptation that probably has been coupled to strong selection on genes involved in detoxification of secondary metabolites. We found that two of the significantly expanded gene families in the painted lady (UDP-glycosyltransferase, carboxylesterase) were associated with detoxification and polyphagy [61, 62, 63]. UDP-glycosyltransferase superfamily includes Lepidoptera-specific subfamilies associated with a variety of functions, such as affinity for plant secondary metabolites [64, 65]. In the painted lady larvae it is upregulated in response to utilization of an extended range of host-plants [26]. Copy-number expansions of these detoxifying gene families could have allowed the painted lady to increase the range of host plants that can be utilized and consequently paved the way for developing the non-diapausing, multigenerational, long-distance migratory lifestyle. The wide range of habitats that long-distance migratory species encounter also probably means that they are exposed to many more different pathogens than sedentary species. Our analysis revealed that the Lepidoptera-specific gene *moricin*, associated with inducible antimicrobial peptides [66], was significantly expanded in the painted lady. An increase in the number of *moricin* copies could have increased the efficiency of defense against a larger suite of pathogens.

The genetic basis of migratory behavior has been investigated in some detail in the monarch butterfly. A combination of approaches has identified candidate genes associated with for example orientation, chemoreception and regulation of the circadian clock [67, 56]. Migratory behavior has evolved independently multiple times within the Lepidoptera clade [68], and the life histories of the monarch butterfly and the painted lady are distinct. However, long-distance migration should put selective pressure on similar traits (e.g. navigation, energy metabolism, muscle endurance), and it is therefore possible that specific gene categories have been under selection in independent lineages. We expanded the analysis to include gene-family expansions that were shared between the two migratory species (the painted lady and the monarch) in our sample set. Significantly expanded gene families were enriched for functions associated with various metabolic processes, defense against pathogens and neuronal activity, all of which are straightforward to associate with migratory behavior intuitively. One gene family with expanded copy numbers in both species and an especially pronounced increase in the painted lady was a family of vacuolar ATPases. The ATPases are ATP-dependent proton pumps involved in membrane transports, and they have been shown to affect for example ion transport in insects [69]. Given the unique expansion of this gene family in both migratory species, we speculate that copy number increase could be involved in flight muscle coordination and/or ion transport for maintenance of homeostasis during long periods of flight.

In this study, we get a first glimpse of the specific genes that have undergone copy number expansions in painted lady specifically and independently in the two migratory species. The functions associated with the expanded gene families can be coupled to the evolution of long-distance migratory behavior. However, further studies on larger species sets with independent migratory and sedentary sister species pairs, in combination with detailed intraspecific population genetic analysis and functional verification experiments will be necessary to dissect the genetic underpinnings of migratory behavior in butterflies in detail.

Patterns of recombination rate variation

Detailed data on recombination rate variation are crucial for understanding the relative effects of random genetic drift and selection on levels of genetic diversity and disentangling the evolutionary forces shaping genetic divergence between incipient species. Understanding how recombination breaks down linkage disequilibrium between physically linked regions is also important for the efficient design of association studies aimed at coupling genetic variation to phenotypic traits. Despite these important contributions to evolutionary genomics research, detailed recombination maps are only available for a handful of butterfly species [70, 32, 30, 71, 35, 72]. In some cases, linkage maps have been used to improve and/or verify the correctness of physical genome assemblies, but analysis of the recombination rate has not been thoroughly assessed in many butterfly species. Here we developed a high-density linkage map based on segregation information in a pedigree with 95 offspring. The map contained $> 1,300$ ordered markers and the overall density was > 3 markers per Mb. Despite being based on a single pedigree, the genetic map developed here revealed a recombination landscape in strong agreement with what has been observed in other butterflies [30, 19](Aleix, Näsvall+Höök+??). This points towards that the painted lady genetic map reflects the historical recombination landscape in the species well.

We estimated the genome-wide average recombination rate in the painted lady to be 3.81 - 4.05 cM / Mb,

dependent on the method applied. The global rate was in the lower end of recombination rate estimates from other Lepidoptera species, which have been in the range from 2.97 - 4.0 cM / Mb in the silkmoth [73, 74] to 5.5 - 6.0 cM / Mb in different Heliconius species [75, 76]. We found a significant negative association between chromosome length and the recombination rate in the painted lady. This is a consistent pattern found across many organism groups and likely a consequence of that at least one crossover event is necessary for correct segregation of chromosomes during meiotic division in the recombining sex, leading to a higher recombination rate per unit length for shorter chromosomes [20, 77, 19]. Butterflies and moths are holocentric, i.e. they lack distinct centromere regions which means that the spindle fibers can attach 'anywhere' along the chromosomes during cell division. This might lead to an expectation of a more uniform distribution of recombination events along chromosomes in holocentric species if crossovers occur randomly. The window-based analysis in the painted lady revealed a bimodal distribution of recombination events along chromosomes, with a significantly higher rate in regions close to, but not directly at, chromosome ends. This distribution is in agreement with previous observations, both in Lepidoptera and in other animals with different centromere types [20, 19]. A possible explanation for this pattern could be mechanical or tension interference between chiasmata when > 1 recombination event occurs on the same chromosome during the same meiotic division [20]. However, in the holocentric *Caenorhabditis elegans*, the number of recombination events is limited to precisely one per chromosome per meiosis, but there is still a strong bimodal pattern of recombination rate variation along chromosomes in this species [78]. An alternative explanation for the bimodal distribution of recombination events along chromosomes could be that synaptonemal complexes are directed towards specific physical positions when the telomeres attach to the nuclear wall [79]. As indicated above, we also found that the recombination rate dropped significantly at the far ends of the chromosomes in the painted lady. This reduced recombination rate at chromosome ends is also consistent with earlier observations and could potentially be attributed to selection against synaptonemal complex formation at chromosome ends, due to a higher risk of ectopic recombination in these generally repeat-rich regions [80].

Since recombination is directly associated with the efficacy of selection, a negative correlation between the regional recombination rate and a number of repeats would be expected if TE insertions predominantly are deleterious. Such associations have been observed in many organisms, although the relationship between TE-abundance and the recombination rate varies to some extent across species and different TE-classes [81, 82]. In the painted lady, we observed a significant positive association between TE-abundance and the regional recombination rate, predominantly driven by a strong effect of SINEs. An explanation for the strong association between SINE density and recombination rate could be SINE-mediated recombination, as has for example been described in humans [83], but we can not exclude other factors affecting both recombination rate and the proliferation efficiency of SINEs. For example, both synaptonemal complexes and SINE insertions might be directed towards regions of more open chromatin structure. One interesting observation was the radically different distribution of TE-classes on the W-chromosome in the painted lady, with a very low frequency of SINEs as compared to the autosomes and the Z-chromosome. Female heterogamety has been conserved across both Lepidoptera and Trichoptera and the lepidopteran W-chromosome probably developed as a result of an ancestral Z-chromosome to autosome fusion > 90 Million years ago [47]. The lack of functional protein coding genes and the significant enrichment of specific TEs suggest that the W-chromosome has been non-recombining over most of that time span. The absence of SINEs on the W-chromosome, and the strong positive association between SINE density and recombination rate on the autosomes and the Z-chromosome, hence suggests that SINEs likely can hijack the recombination machinery and mediate their own proliferation via double-strand breaks.

We observed a negative association between the recombination rate and gene density. This is in contrast with results from similar studies in other organism groups [84, 85] - likely a consequence of the strong association between recombination rate and chromosome size, since the association with gene density was insignificant when chromosome size was included as an explanatory variable. The observed weak positive association between GC-content and recombination is in agreement with the limited effect of GC-biased gene conversion (gBGC) in butterflies [86]. We did not find any association between recombination rate and the presence of extended orthogroups, which would be expected if gene duplication is associated with unequal crossing-over. This could possibly be a consequence of the more efficient removal of deleterious duplications in regions with higher recombination. However, repetitive elements can trigger ectopic recombination which can explain the observed significant positive association between gene gains and density of LTRs, LINEs and DNA elements in the painted lady.

Conclusions

In this study, we present detailed annotation and recombination rate information for the painted lady butterfly (*Vanessa cardui*), a species with exceptional life-history traits such as long distance migration, continuous direct development and an unmatched capacity to utilize different types of larval host plants. We analyzed lineage-specific gene family expansions and found that expanded genes were mainly associated with fat and protein metabolism, detoxification and defense against pathogens. A detailed TE-annotation revealed that several TE-classes were positively associated with the presence of gained genes, potentially indicating their involvement in ectopic recombination. Recombination rate variation was negatively associated with chromosome size and positively associated with the proportion of short interspersed elements (SINEs). We conclude that the genome structure of the painted lady is shaped by a complex interplay between recombination, gene duplications and repeat activity and provide the first set of candidate genes potentially involved in the evolution of migratory behavior in this cosmopolitan butterfly species.

Methods

Linkage map

Sampling and DNA-extraction

Offspring from one painted lady female were reared on thistles (*Cirsium vulgare*) in the greenhouse until pupation. The bursa copulatrix of the female was examined and only one spermatophore was detected, indicating that a single male had sired all offspring. The offspring were snap frozen in liquid nitrogen and stored in $-20°$C until DNA extraction. DNA was extracted from thorax tissue of the female and an abdominal segment of the offspring pupae, using a modified high salt extraction method [87]. The quality of the DNA was analyzed with Nanodrop (ThermoFischer Scientific) and the yield was quantified with Qubit (ThermoFischer Scientific). Extracted DNA was digested with the restriction enzyme EcoR1 according to the manufacturer's protocol, using 16 hours digestion time (ThermoFischer Scientific). DNA fragmentation was verified with standard gel electrophoresis. Digested DNA from 95 offspring with the highest yield and the dam was shipped to the National Genomics Infrastructure (NGI, see acknowledgements) in Stockholm for library preparation (standard protocol), individual barcoding and multiplex sequencing using 2×151 bp paired-end reads on one NovaSeq6000 S4 lane.

Sequence data processing

The quality of the raw reads was assessed with FastQC [88]. The reads were filtered using the Stacks2 modules `clone_filter` to remove PCR-duplicates and `process_radtags` to remove reads if the average phredscore dropped below 10 in any window 15% of the length of the read [89]. Removal of reads with unassigned bases and truncation to 125 bp was done using option `-c`, and `--disable_rad_chec` was applied to keep reads with incomplete RAD-tags.

We mapped the filtered reads to the genome assembly produced by the Darwin Tree of Life initiative (available in the NCBI database, genome `GCA_905220365.1_ilVanCard2.1_genomic.fna.gz`, accessed 13/03/2021) using the bwa mem algorithm [90] with default options. Resulting bam files were sorted with samtools sort [91] and filtered with `samtools view {q 10` (only keep reads with mapping quality score above 10). A custom script was applied to retain reads with unique hits only. The mapping coverage was analyzed with Qualimap [92]. The offspring were defined as females if the coverage on the Z-chromosome was <75% of the average coverage over all chromosomes and as males if the coverage was > 75%. Samtools mpileup was used for variant calling using minimum mapping quality (`-q`) 10 and minimum base quality (`-Q`) 10 [91]. The variants were then converted to likelihoods with Pileup2Likelihoods in LepMap3 using default settings [93].

Building the linkage map

LepMap3 was used to construct the linkage map [93]. The module ParentCall calls informative parental markers and uses genotype likelihood information from the offspring to impute missing or erroneous parental markers. This module was run with default values, except that non-informative markers were removed and `zLimit = 2`, which was applied to detect markers segregating as sex chromosomes. Markers mapping to the W-chromosome, mitochondria or to repeats were removed with BEDTools [94]. The markers were assigned to linkage groups using SeparateChromosomes2 with `lodDifference=2` and `distortionLod=1`. The LOD-limit was estimated empirically by testing a range of LODscores (1-30) and finally set to 24, which resulted in the expected number (31) of linkage groups. To assign additional unlinked markers to the linkage groups, JoinSingles was run with `lodLimits = 18`.

OrderMarkers was run over 50 iterations for each linkage group to determine the most likely distance between the markers and the maps with the highest likelihood were selected for further refinement. Since butterflies have female achiasmy, we limited the analysis to markers that were informative only in males (`informativeMask=1`) or in both sexes (`informativeMask=13`). To account for partial interference the Kosambi distance method was applied. The trimmed map was reevaluated with OrderMarkers with the options `evaluateOrder` and

`improveOrder=1`. The maps were thinned so that only SNPs > 300 bp apart were retained (i.e. at least one SNP per RAD-tag). Any remaining unlinked markers at linkage group ends were manually removed after visual inspection and the final maps were once more reevaluated with OrderMarkers. Collinearity between physical and genetic positions were tested with Pearson's product moment correlation as implemented in `cor.test` in R [95].

Genome annotation and whole genome statistics

Genome assembly statistics

With very few exceptions, the order of markers in the linkage map was in agreement with the physical order in the assembly. We therefore did not make any corrections to the physical assembly before further analysis. Standard genome assembly summary statistics were calculated for the genome assembly after linkage map verification, using the QUAST suite [96]. For the subsequent analysis we excluded unassembled haplotigs from the genome assembly and retained all the other scaffolds.

We used MCScanX [97] to detect syntenic blocks between the painted lady genome assembly on the one hand and the silkmoth and the the postman butterfly on the other. We downloaded the annotation for the silkmoth assembly from SilkBase (/https://silkdb.bioinfotoolkits.net/) and the 2.5-version of the postman annotation from LepBase (download.lepbase.org/v4/, downloaded 2021-06-21). BLAST was used for primary alignment and we used a custom script to select the five hits with the highest E-values and use them as input for the MCScanX. The CIRCOS library [98] was used for visualization of the results. Gene and repeat annotation The annotation of the painted lady genome assembly was performed using MAKER version 3.00.0 [99] iteratively in three steps. In the first step, we mapped previously available transcriptomic evidence data from the painted lady based on wing tissue [28](accessed on 2020-05-15) and masked all known repeats. RepeatMasker version 4.0.3 [100] was used within the MAKER pipeline with a manually curated Lepidoptera repeat library [15] serving as a reference. The first MAKER produced a set of gene models, which were quality controlled using Annotation Edit Distance (AED) statistics. AED quantifies congruency between a gene annotation and its supporting evidence. We discarded gene models with AED scores higher than 0.5 (50% of the gene model length not matching corresponding evidence sequence) using custom scripts. The retained gene models were provided as a training set for the second run of MAKER.

The second iteration of MAKER was run to generate gene models using the ab-initio gene predicting algorithm implemented in SNAP [101]. For the last step in the MAKER pipeline, gene models predicted by SNAP and additional protein evidence from the Uniprot database (https://www.uniprot.org/; accessed 2021-04-01) were used. A set of Lepidoptera proteins from the Swiss-prot section of the Uniprot database were downloaded and manually curated. All genes from the curated set were included while only fully sequenced nuclear proteins with predicted functions from the non-curated gene set were included (custom scripts were used for selection). This selection resulted in 36,907 proteins. Finally, all obtained evidence and ab initio predicted genes were merged resulting in 18,860 gene models. Resulting genes were renamed using MAKER supplementary scripts.

Additional curation and W-chromosome

The gene models constructed by MAKER were filtered based on standard options; discarding gene models with AED and eAED scores <0.5 and/or length < 50 amino acids. To search for functional domains in putative genes, we used InterProScan with default settings [102]. A number of TE-related domains were detected within gene models indicating a need for a more detailed transposable element annotation. The repeat library was extended by adding evidence from the current RepBase for all Arthoropoda [103] and curated repeats from the monarch butterfly [104] and ran RepeatModeller for the painted lady. RepeatMasker was thereafter run again with the updated repeat database. The repeat annotation file from RepeatMasker was used for downstream analysis.

Coordinates of newly identified repeats were intersected with gene model positions using BEDTools [94] and removed gene models that overlapped more than 50% of the length of a repeat. We then searched for keywords in the InterProScan domain output and removed genes containing at least one TE domain. For the W-chromosome, we manually curated the InterProScan output and found no functional information for any genes. The filtering resulted in a set of 13,161 genes, including 12,209 genes with preliminary assignments in eggnog [105]. The entire painted lady gene set represented 89.9% of the complete BUSCO arthropod gene set [106].

Gene family evolution

We investigated gene family evolution in the painted lady by comparing our obtained gene annotations with other annotated nymphalid genomes available on Lepbase. Protein fasta files for eight other nymphalid species - squinting bush brown (*Bicyclus anynana*), monarch (*Danaus plexippus*), postman (*Heliconius melpomene melpomene*), red postman (*Heliconius erato lativitta*), common buckeye (*Junonia coenia*),

ringlet (*Maniola hyperantus*), speckled wood (*Pararge aegeria*) and Kamehameha butterfly *(Vanessa tameamea)* - were downloaded from Lepbase (http://download.lepbase.org/v4/sequence/: accessed 2021-06-21; Supplementary Table S1). The annotated gene sets in each species were filtered to only include one transcript per gene. To cluster the annotated genes into orthogroups and infer species specific orthogroups and gene duplications, OrthoFinder/2.5.2 [107] was used with default settings. The total gene counts for each orthogroup and species from OrthoFinder was used as input to estimate gene family expansions and contractions with the software BadiRate, using the maximum likelihood option and the birth/death/innovation (BDI) model [108]. We used the species tree obtained with OrthoFinder as input, with additional conversions using Tree as implemented in ete3 [109].

For each orthogroup identified in OrthoFinder, different models reflecting the evolution of the gene families were tested. The null model (Global rate model) assumes a uniform rate of gene gains/losses for all branches in the provided species tree. Alternative models were specified as follows; i) to detect gene family changes specific to the painted lady, a distinct branch rate was specified in the painted lady with all the other branches evolving at uniform, background rates, and, ii) the terminal branches of the two distinct migratory species, the painted lady and the monarch, were set at a common rate, differing from all other taxa in the data set. The rationale behind the last setting was to allow for identification of gene family expansions unique to migratory butterflies. Each model was run twice and the replicate with highest likelihood for each model was used for model comparisons.

Likelihoods of all models were compared using Aikaike's Information Criterion (AIC) [110], calculated as $2K - 2\log L$, where K is the number of parameters and $\log L$ is the logarithm of the likelihood of the model. The orthogroups where the alternative models in BadiRate inferred gene gains > 0 with the lowest AIC, were used for analysis of functional enrichment. BadiRate was partly run with a modified version of the R-package BadiRateR (BadiRate) and custom scripts. We visualized the genomic location of genes belonging to extended orthogroups identified in BadiRate with custom bash scripts and PhenoGram [111], using gene names and positions from the annotation gff file. Gene ontology enrichment Potential enrichment of functional categories in the significantly expanded gene sets was analyzed using the Bioconductor package topGO version 2.44.0 [112] in R version 4.1.0 [95]. A custom database was generated based on the annotated gene set with gene ontology (GO) terms associated to the categories biological process, cellular component and molecular function. Since the gene set of interest is based on gene counts, the enrichment test was performed with Fisher's exact test using the default algorithm (`\weight01"`) which accounts for the hierarchical structure of the GO-terms [113]. This means that the resulting tests were not completely independent and correcting for multiple testing might be over-conservative. We still adjusted the p-values with Benjamini-Hochberg's method of multiple test correction [114].

Recombination rate analysis

Chromosome level analysis

Global and chromosome-specific recombination rates were estimated by dividing the linkage map length (unit = cM) with the physical length (bp) of the corresponding part (whole genome or individual chromosome) of the physical genome assembly. Regional recombination rates were estimated with local linear regression in 2 Mb non-overlapping windows containing 2 or more markers using the R-package MareyMap [115].

Window-based analysis

We quantified the spatial distribution of various genomic features along the painted lady genome using custom scripts. Positions of the specific TE classes were accessed from the RepeatMaker output file and positions of genes were taken from the annotation file from MAKER. For each 2 Mb window, we calculated the density (fraction of window covered by element / window length) of genes, TEs in total, LTRs, SINEs, LINEs and DNA-transposons with in-house developed scripts. For the genes belonging to extended orthogroups, we integrated the list of the extended orthogroups from BadiRate, gene names from Orthofinder and positions from MAKER. All 2 Mb windows of the genome were assigned to bins; one bin containing windows without gene gains and the other with windows containing at least one gene. Potential differences in densities of genomic features between bins were assessed with two-sided Wilcoxon rank sum tests in R [116]. Associations between genomic features and the recombination rate To characterize the associations between recombination rate and specific genomic elements, correlation tests were performed with the cor.test function in R using Spearman's rank correlation [117], after testing for deviation from normal distribution with the Shapiro-Wilk normality test [118]. We then applied the `lm` function in R to explore the relationships between the recombination rate as response variable and chromosome length, relative position on the chromosome, density of genes, density of different repeat classes, and GC-content as explanatory variables. Prior to the latter analysis, explanatory

variables were scaled and centered, by subtracting the mean and dividing by the standard deviation of the variable. We used the R-package `ggplot2` for visualizations [119].

Acknowledgements

Financial support for this project was provided by FORMAS (Research grant 2019-00670 to N.B.) and The Swedish Collegium for Advanced Science (Natural Sciences Programme, Knut and Alice Wallenberg Foundation, Postdoc funding for D.S.). The authors acknowledge support from the National Genomics Infrastructure in Stockholm funded by Science for Life Laboratory, the Knut and Alice Wallenberg Foundation and the Swedish Research Council, and SNIC/Uppsala Multidisciplinary Center for Advanced Computational Science for assistance with massively parallel sequencing and access to the UPPMAX computational infrastructure. Data access Competing interest statement

Author details

[1]Department of Ecology and Genetics, Uppsala University, Norbyvägen 18D, 75236 Uppsala, Sweden. [2] Swedish Collegium for Advanced Study, Thunbergsvägen 2, 75236, Uppsala, Sweden. [3] The Butterfly Diversity and Evolution Lab, Institut de Biologia Evolutiva, Passeig Marítim de la Barceloneta 37-49, 08003, Barcelona, Spain. [4] Institut Botànic de Barcelona (IBB, CSIC), Passeig del Migdia s/n, 08038, Barcelona, Spain. [5] authors contributed equally).

References

1. Henikoff, S.: Gene Families: The Taxonomy of Protein Paralogs and Chimeras **278**(5338), 609–614. doi:10.1126/science.278.5338.609. Accessed 2021-09-28
2. Ojeda-López, J., Marczuk-Rojas, J.P., Polushkina, O.A., Purucker, D., Salinas, M., Carretero-Paulet, L.: Evolutionary analysis of the Moringa oleifera genome reveals a recent burst of plastid to nucleus gene duplications **10**(1), 17646. doi:10.1038/s41598-020-73937-w. Accessed 2021-06-11
3. Zhang, L.: Does Recombination Shape the Distribution and Evolution of Tandemly Arrayed Genes (TAGs) in the Arabidopsis thaliana Genome? **13**(12), 2533–2540. doi:10.1101/gr.1318503. Accessed 2022-03-21
4. Chen, S., Krinsky, B.H., Long, M.: New genes as drivers of phenotypic evolution **14**(9), 645–660. doi:10.1038/nrg3521. Accessed 2022-03-22
5. Kondrashov, F.A.: Gene duplication as a mechanism of genomic adaptation to a changing environment **279**(1749), 5048–5057. doi:10.1098/rspb.2012.1108. Accessed 2021-09-27
6. Schwander, T., Libbrecht, R., Keller, L.: Supergenes and Complex Phenotypes **24**(7), 288–294. doi:10.1016/j.cub.2014.01.056. Accessed 2022-03-22
7. McClintock, B.: Controlling Elements and the Gene **21**(0), 197–216. doi:10.1101/SQB.1956.021.01.017. Accessed 2022-03-23
8. Kazazian, H.H.: Mobile Elements: Drivers of Genome Evolution **303**(5664), 1626–1632. doi:10.1126/science.1089670. Accessed 2021-09-28
9. Kidwell, M.G., Lisch, D.: Transposable elements as sources of variation in animals and plants **94**(15), 7704–7711. doi:10.1073/pnas.94.15.7704. Accessed 2021-09-28
10. Van't Hof, A.E., Campagne, P., Rigden, D.J., Yung, C.J., Lingley, J., Quail, M.A., Hall, N., Darby, A.C., Saccheri, I.J.: The industrial melanism mutation in British peppered moths is a transposable element **534**(7605), 102–105. doi:10.1038/nature17951. 27251284
11. Hedges, D.J., Deininger, P.L.: Inviting instability: Transposable elements, double-strand breaks, and the maintenance of genome integrity **616**(1-2), 46–59. doi:10.1016/j.mrfmmm.2006.11.021. Accessed 2021-09-28
12. Wells, J.N., Feschotte, C.: A Field Guide to Eukaryotic Transposable Elements **54**(1), 539–561. doi:10.1146/annurev-genet-040620-022145. Accessed 2021-09-28
13. Ray, D.A., Grimshaw, J.R., Halsey, M.K., Korstian, J.M., Osmanski, A.B., Sullivan, K.A.M., Wolf, K.A., Reddy, H., Foley, N., Stevens, R.D., Knisbacher, B.A., Levy, O., Counterman, B., Edelman, N.B., Mallet, J.: Simultaneous TE Analysis of 19 Heliconiine Butterflies Yields Novel Insights into Rapid TE-Based Genome Diversification and Multiple SINE Births and Deaths **11**(8), 2162–2177. doi:10.1093/gbe/evz125. Accessed 2021-09-28
14. Podsiadlowski, L., Tunström, K., Espeland, M., Wheat, C.W.: The Genome Assembly and Annotation of the Apollo Butterfly Parnassius apollo, a Flagship Species for Conservation Biology **13**(8), 122. doi:10.1093/gbe/evab122. Accessed 2022-03-22
15. Talla, V., Suh, A., Kalsoom, F., Dincă, V., Vila, R., Friberg, M., Wiklund, C., Backström, N.: Rapid Increase in Genome Size as a Consequence of Transposable Element Hyperactivity in Wood-White (Leptidea) Butterflies **9**(10), 2491–2505. doi:10.1093/gbe/evx163. Accessed 2020-01-09
16. Peñalba, J.V., Wolf, J.B.W.: From molecules to populations: Appreciating and estimating recombination rate variation **21**(8), 476–492. doi:10.1038/s41576-020-0240-1. Accessed 2021-09-28
17. Stapley, J., Feulner, P.G.D., Johnston, S.E., Santure, A.W., Smadja, C.M.: Variation in recombination frequency and distribution across eukaryotes: Patterns and processes **372**(1736), 20160455. doi:10.1098/rstb.2016.0455. 29109219
18. Tiley, G.P., Burleigh, J.G.: The relationship of recombination rate, genome structure, and patterns of molecular evolution across angiosperms **15**(1), 194. doi:10.1186/s12862-015-0473-3. Accessed 2022-03-22
19. Martin, S.H., Davey, J.W., Salazar, C., Jiggins, C.D.: Recombination rate variation shapes barriers to introgression across butterfly genomes **17**(2), 2006288. doi:10.1371/journal.pbio.2006288. Accessed 2020-04-30
20. Haenel, Q., Laurentino, T.G., Roesti, M., Berner, D.: Meta-analysis of chromosome-scale crossover rate variation in eukaryotes and its significance to evolutionary genomics **27**(11), 2477–2497. doi:10.1111/mec.14699. Accessed 2021-09-24
21. Talla, V., Soler, L., Kawakami, T., Dincă, V., Vila, R., Friberg, M., Wiklund, C., Backström, N.: Dissecting the Effects of Selection and Mutation on Genetic Diversity in Three Wood White (Leptidea) Butterfly Species **11**(10), 2875–2886. doi:10.1093/gbe/evz212. Accessed 2020-04-30
22. Talavera, G., Bataille, C., Benyamini, D., Gascoigne-Pees, M., Vila, R.: Round-trip across the Sahara: Afrotropical Painted Lady butterflies recolonize the Mediterranean in early spring **14**(6), 20180274. doi:10.1098/rsbl.2018.0274. Accessed 2021-09-28
23. Stefanescu, C., Soto, D.X., Talavera, G., Vila, R., Hobson, K.A.: Long-distance autumn migration across the Sahara by painted lady butterflies: Exploiting resource pulses in the tropical savannah **12**(10), 20160561. doi:10.1098/rsbl.2016.0561. Accessed 2022-02-22
24. Talavera, G., Vila, R.: Discovery of mass migration and breeding of the painted lady butterfly Vanessa cardui in the Sub-Sahara: The Europe–Africa migration revisited **2016**(n/a). doi:10.1111/bij.12873. Accessed 2022-03-22
25. Garcia-Berro, A., Talla, V., Vila, R., Wai, H.K., Shipilina, D., Chan, K.G., Pierce, N.E., Backström, N., Talavera, G.: Genomic demographic inference shows migratory butterflies display higher heterozygosity and long-term effective population size. (in prep)
26. Celorio-Mancera, M.d.l.P., Wheat, C.W., Huss, M., Vezzi, F., Neethiraj, R., Reimegård, J., Nylin, S., Janz, N.: Evolutionary history of host use, rather than plant phylogeny, determines gene expression in a generalist butterfly **16**(1), 59. doi:10.1186/s12862-016-0627-y. Accessed 2020-01-08
27. Merlin, C., Liedvogel, M.: The genetics and epigenetics of animal migration and orientation: Birds, butterflies and beyond **222**. doi:10.1242/jeb.191890
28. Connahs, H., Rhen, T., Simmons, R.B.: Transcriptome analysis of the painted lady butterfly, Vanessa cardui during wing color pattern development **17**(1), 270. doi:10.1186/s12864-016-2586-5. Accessed 2022-03-22
29. Zhang, L., Steward, R.A., Wheat, C.W., Reed, R.D.: High-Quality Genome Assembly and Comprehensive Transcriptome of the Painted Lady Butterfly Vanessa cardui **13**(7). doi:10.1093/gbe/evab145. Accessed 2021-11-22
30. Davey, J.W., Barker, S.L., Rastas, P.M., Pinharanda, A., Martin, S.H., Durbin, R., McMillan, W.O., Merrill, R.M., Jiggins, C.D.: No

evidence for maintenance of a sympatric Heliconius species barrier by chromosomal inversions **1**(3), 138–154. doi:10.1002/evl3.12. Accessed 2022-03-22

31. Ahola, V., Lehtonen, R., Somervuo, P., Salmela, L., Koskinen, P., Rastas, P., Välimäki, N., Paulin, L., Kvist, J., Wahlberg, N., Tanskanen, J., Hornett, E.A., Ferguson, L.C., Luo, S., Cao, Z., de Jong, M.A., Duplouy, A., Smolander, O.-P., Vogel, H., McCoy, R.C., Qian, K., Chong, W.S., Zhang, Q., Ahmad, F., Haukka, J.K., Joshi, A., Salojärvi, J., Wheat, C.W., Grosse-Wilde, E., Hughes, D., Katainen, R., Pitkänen, E., Ylinen, J., Waterhouse, R.M., Turunen, M., Vähärautio, A., Ojanen, S.P., Schulman, A.H., Taipale, M., Lawson, D., Ukkonen, E., Mäkinen, V., Goldsmith, M.R., Holm, L., Auvinen, P., Frilander, M.J., Hanski, I.: The Glanville fritillary genome retains an ancient karyotype and reveals selective chromosomal fusions in Lepidoptera **5**(1), 4737. doi:10.1038/ncomms5737. Accessed 2022-03-22
32. Celorio-Mancera, M.d.l.P., Rastas, P., Steward, R.A., Nylin, S., Wheat, C.W.: Chromosome level assembly of the comma butterfly (Polygonia c-album). doi:10.1093/gbe/evab054. Accessed 2021-04-06
33. Gu, L., Reilly, P.F., Lewis, J.J., Reed, R.D., Andolfatto, P., Walters, J.R.: Dichotomy of Dosage Compensation along the Neo Z Chromosome of the Monarch Butterfly **29**(23), 4071–40773. doi:10.1016/j.cub.2019.09.056. 31735674. Accessed 2022-03-22
34. Li, X., Fan, D., Zhang, W., Liu, G., Zhang, L., Zhao, L., Fang, X., Chen, L., Dong, Y., Chen, Y., Ding, Y., Zhao, R., Feng, M., Zhu, Y., Feng, Y., Jiang, X., Zhu, D., Xiang, H., Feng, X., Li, S., Wang, J., Zhang, G., Kronforst, M.R., Wang, W.: Outbred genome sequencing and CRISPR/Cas9 gene editing in butterflies **6**(1), 8212. doi:10.1038/ncomms9212. Accessed 2021-09-28
35. Smolander, O.-P., Blande, D., Ahola, V., Rastas, P., Tanskanen, J., Kammonen, J.I., Oostra, V., Pellegrini, L., Ikonen, S., Dallas, T., DiLeo, M.F., Duplouy, A., Duru, I.C., Halimaa, P., Kahilainen, A., Kuwar, S.S., Kärenlampi, S.O., Lafuente, E., Luo, S., Makkonen, J., Nair, A., de la Paz Celorio-Mancera, M., Pennanen, V., Ruokolainen, A., Sundell, T., Tervahauta, A.I., Twort, V., van Bergen, E., Österman-Udd, J., Paulin, L., Frilander, M.J., Auvinen, P., Saastamoinen, M.: Improved chromosome-level genome assembly of the Glanville fritillary butterfly (Melitaea cinxia) integrating Pacific Biosciences long reads and a high-density linkage map **11**(1), 097. doi:10.1093/gigascience/giab097. 35022701
36. Yang, J., Wan, W., Xie, M., Mao, J., Dong, Z., Lu, S., He, J., Xie, F., Liu, G., Dai, X., Chang, Z., Zhao, R., Zhang, R., Wang, S., Zhang, Y., Zhang, W., Wang, W., Li, X.: Chromosome-level reference genome assembly and gene editing of the dead-leaf butterfly *Kallima inachus* **20**(4), 1080–1092. doi:10.1111/1755-0998.13185. Accessed 2021-09-28
37. Hill, J., Rastas, P., Hornett, E.A., Neethiraj, R., Clark, N., Morehouse, N., de la Paz Celorio-Mancera, M., Cols, J.C., Dircksen, H., Meslin, C., Keehnen, N., Pruisscher, P., Sikkink, K., Vives, M., Vogel, H., Wiklund, C., Woronik, A., Boggs, C.L., Nylin, S., Wheat, C.W.: Unprecedented reorganization of holocentric chromosomes provides insights into the enigma of lepidopteran chromosome evolution **5**(6), 3648. doi:10.1126/sciadv.aau3648. Accessed 2022-03-15
38. Van Belleghem, S.M., Rastas, P., Papanicolaou, A., Martin, S.H., Arias, C.F., Supple, M.A., Hanly, J.J., Mallet, J., Lewis, J.J., Hines, H.M., Ruiz, M., Salazar, C., Linares, M., Moreira, G.R.P., Jiggins, C.D., Counterman, B.A., McMillan, W.O., Papa, R.: Complex modular architecture around a simple toolkit of wing pattern genes **1**(3), 1–12. doi:10.1038/s41559-016-0052. Accessed 2021-11-08
39. Lukhtanov, V.: The blue butterfly Polyommatus (Plebicula) atlanticus (Lepidoptera, Lycaenidae) holds the record of the highest number of chromosomes in the non-polyploid eukaryotic organisms **9**(4), 683–690. doi:10.3897/CompCytogen.v9i4.5760. Accessed 2022-03-14
40. de Vos, J.M., Augustijnen, H., Bätscher, L., Lucek, K.: Speciation through chromosomal fusion and fission in Lepidoptera **375**(1806), 20190539. doi:10.1098/rstb.2019.0539. Accessed 2022-03-14
41. Challi, R.J., Kumar, S., Dasmahapatra, K.K., Jiggins, C.D., Blaxter, M.: Lepbase: The Lepidopteran genome database, 056994. doi:10.1101/056994. Accessed 2022-03-23
42. Li, F., Zhao, X., Li, M., He, K., Huang, C., Zhou, Y., Li, Z., Walters, J.R.: Insect genomes: Progress and challenges **28**(6), 739–758. doi:10.1111/imb.12599. Accessed 2020-11-09
43. Lewis, J.J., Cicconardi, F., Martin, S.H., Reed, R.D., Danko, C.G., Montgomery, S.H.: The Dryas iulia Genome Supports Multiple Gains of a W Chromosome from a B Chromosome in Butterflies **13**(7). doi:10.1093/gbe/evab128. Accessed 2021-10-28
44. Mita, K., Kasahara, M., Sasaki, S., Nagayasu, Y., Yamada, T., Kanamori, H., Namiki, N., Kitagawa, M., Yamashita, H., Yasukochi, Y., Kadono-Okuda, K., Yamamoto, K., Ajimura, M., Ravikumar, G., Shimomura, M., Nagamura, Y., Shin-i, T., Abe, H., Shimada, T., Morishita, S., Sasaki, T.: The Genome Sequence of Silkworm, Bombyx mori **11**(1), 27–35. doi:10.1093/dnares/11.1.27. Accessed 2022-03-23
45. Abe, H., Fujii, T., Tanaka, N., Yokoyama, T., Kakehashi, H., Ajimura, M., Mita, K., Banno, Y., Yasukochi, Y., Oshiki, T., Nenoi, M., Ishikawa, T., Shimada, T.: Identification of the female-determining region of the W chromosome in Bombyx mori **133**(3), 269–282. doi:10.1007/s10709-007-9210-1. Accessed 2022-03-23
46. Bachtrog, D.: Y chromosome evolution: Emerging insights into processes of Y chromosome degeneration **14**(2), 113–124. doi:10.1038/nrg3366. 23329112. Accessed 2022-03-23
47. Fraïsse, C., Picard, M.A.L., Vicoso, B.: The deep conservation of the Lepidoptera Z chromosome suggests a non-canonical origin of the W **8**(1), 1486. doi:10.1038/s41467-017-01663-5. Accessed 2022-03-23
48. Lipinski, K.J., Farslow, J.C., Fitzpatrick, K.A., Lynch, M., Katju, V., Bergthorsson, U.: High Spontaneous Rate of Gene Duplication in Caenorhabditis elegans **21**(4), 306–310. doi:10.1016/j.cub.2011.01.026. 21295484. Accessed 2021-09-27
49. Loehlin, D.W., Carroll, S.B.: Expression of tandem gene duplicates is often greater than twofold **113**(21), 5988–5992. doi:10.1073/pnas.1605886113. 27162370. Accessed 2021-09-27
50. Emerson, J.J., Cardoso-Moreira, M., Borevitz, J.O., Long, M.: Natural Selection Shapes Genome-Wide Patterns of Copy-Number Polymorphism in Drosophila melanogaster **320**(5883), 1629–1631. doi:10.1126/science.1158078. Accessed 2021-09-27
51. Shields, O.: Journal of the Lepidopterists' Society. `https://www.biodiversitylibrary.org/item/128069`
52. Stefanescu, C., Páramo, F., Åkesson, S., Alarcón, M., Ávila, A., Brereton, T., Carnicer, J., Cassar, L.F., Fox, R., Heliölä, J., Hill, J.K., Hirneisen, N., Kjellén, N., Kühn, E., Kuussaari, M., Leskinen, M., Liechti, F., Musche, M., Regan, E.C., Reynolds, D.R., Roy, D.B., Ryrholm, N., Schmaljohann, H., Settele, J., Thomas, C.D., van Swaay, C., Chapman, J.W.: Multi-generational long-distance migration of insects: Studying the painted lady butterfly in the Western Palaearctic **36**(4), 474–486. doi:10.1111/j.1600-0587.2012.07738.x. Accessed 2022-03-23
53. HOSTS, h.n.a.u.-s.d.: HOSTS - a Database of the World's Lepidopteran Hostplants. `https://www.nhm.ac.uk/our-science/data/hostplants/search/index.dsml`
54. Nylin, S., Slove, J., Janz, N.: HOST PLANT UTILIZATION, HOST RANGE OSCILLATIONS AND DIVERSIFICATION IN NYMPHALID BUTTERFLIES: A PHYLOGENETIC INVESTIGATION: HOST RANGE OSCILLATIONS IN BUTTERFLIES **68**(1), 105–124. doi:10.1111/evo.12227. Accessed 2020-01-08
55. Kang, L., Chen, X., Zhou, Y., Liu, B., Zheng, W., Li, R., Wang, J., Yu, J.: The analysis of large-scale gene expression correlated to the phase changes of the migratory locust **101**(51), 17611–17615. doi:10.1073/pnas.0407753101. Accessed 2022-03-23
56. Zhu, H., Gegear, R.J., Casselman, A., Kanginakudru, S., Reppert, S.M.: Defining behavioral and molecular differences between summer and migratory monarch butterflies **7**(1), 14. doi:10.1186/1741-7007-7-14. Accessed 2022-03-23
57. Landys, M.M., Piersma, T., Guglielmo, C.G., Jukema, J., Ramenofsky, M., Wingfield, J.C.: Metabolic profile of long-distance migratory flight and stopover in a shorebird **272**(1560), 295–302. doi:10.1098/rspb.2004.2952. 15705555. Accessed 2022-03-02
58. Murata, M., Tojo, S.: Utilization of lipid for flight and reproduction in Spodoptera litura (Lepidoptera: Noctuidae) **99**(2), 221–224. doi:10.14411/eje.2002.031. Accessed 2022-03-02
59. Srygley, R.B., Dudley, R.: Optimal strategies for insects migrating in the flight boundary layer: Mechanisms and consequences **48**(1),

119–133. doi:10.1093/icb/icn011. Accessed 2022-03-02
60. Weber, J.-M.: The physiology of long-distance migration: Extending the limits of endurance metabolism **212**(5), 593–597. doi:10.1242/jeb.015024. Accessed 2022-03-02
61. Breeschoten, T., van der Linden, C.F.H., Ros, V.I.D., Schranz, M.E., Simon, S.: Expanding the Menu: Are Polyphagy and Gene Family Expansions Linked across Lepidoptera? **14**(1), 283. doi:10.1093/gbe/evab283. Accessed 2022-03-24
62. Hatfield, M.J., Umans, R.A., Hyatt, J.L., Edwards, C.C., Wierdl, M., Tsurkan, L., Taylor, M.R., Potter, P.M.: Carboxylesterases: General detoxifying enzymes **259**, 327–331. doi:10.1016/j.cbi.2016.02.011. 26892220. Accessed 2022-02-21
63. Nagare, M., Ayachit, M., Agnihotri, A., Schwab, W., Joshi, R.: Glycosyltransferases: The multifaceted enzymatic regulator in insects **30**(2), 123–137. doi:10.1111/imb.12686. 33263941
64. Huang, F.-F., Chai, C.-L., Zhang, Z., Liu, Z.-H., Dai, F.-Y., Lu, C., Xiang, Z.-H.: The UDP-glucosyltransferase multigene family in Bombyx mori **9**, 563. doi:10.1186/1471-2164-9-563. 19038024. Accessed 2022-02-21
65. Luque, T., Okano, K., O'Reilly, D.R.: Characterization of a novel silkworm (Bombyx mori) phenol UDP-glucosyltransferase **269**(3), 819–825. doi:10.1046/j.0014-2956.2001.02723.x. Accessed 2022-02-21
66. Hara, S., Yamakawa, M.: Moricin, a novel type of antibacterial peptide isolated from the silkworm, Bombyx mori **270**(50), 29923–29927. doi:10.1074/jbc.270.50.29923. 8530391
67. Zhan, S., Zhang, W., Niitepõld, K., Hsu, J., Haeger, J.F., Zalucki, M.P., Altizer, S., de Roode, J.C., Reppert, S.M., Kronforst, M.R.: The genetics of monarch butterfly migration and warning colouration **514**(7522), 317–321. doi:10.1038/nature13812. Accessed 2022-03-23
68. Chowdhury, S., Fuller, R.A., Dingle, H., Chapman, J.W., Zalucki, M.P.: Migration in butterflies: A global overview **96**(4), 1462–1483. doi:10.1111/brv.12714. Accessed 2022-03-24
69. Wieczorek, H., Beyenbach, K.W., Huss, M., Vitavska, O.: Vacuolar-type proton pumps in insect epithelia **212**(11), 1611–1619. doi:10.1242/jeb.030007. 19448071. Accessed 2022-02-21
70. Beldade, P., Saenko, S.V., Pul, N., Long, A.D.: A Gene-Based Linkage Map for Bicyclus anynana Butterflies Allows for a Comprehensive Analysis of Synteny with the Lepidopteran Reference Genome **5**(2), 1000366. doi:10.1371/journal.pgen.1000366. Accessed 2020-04-30
71. Rosser, N., Edelman, N.B., Queste, L.M., Nelson, M., Seixas, F., Dasmahapatra, K.K., Mallet, J.: Complex basis of hybrid female sterility and Haldane's rule in Heliconius butterflies: Z-linkage and epistasis (31). doi:10.1111/mec.16272. Accessed 2021-12-06
72. Tunström, K., Woronik, A., Hanly, J.J., Rastas, P., Chichvarkhin, A., Warren, A.D., Kawahara, A., Schoville, S.D., Ficarrotta, V., Porter, A.H., Watt, W.B., Martin, A., Wheat, C.W.: A complex interplay between balancing selection and introgression maintains a genus-wide alternative life history strategy, 2021–0520445023. doi:10.1101/2021.05.20.445023. Accessed 2022-03-23
73. Yamamoto, K., Nohata, J., Kadono-Okuda, K., Narukawa, J., Sasanuma, M., Sasanuma, S.-i., Minami, H., Shimomura, M., Suetsugu, Y., Banno, Y., Osoegawa, K., de Jong, P.J., Goldsmith, M.R., Mita, K.: A BAC-based integrated linkage map of the silkworm Bombyx mori **9**(1), 21. doi:10.1186/gb-2008-9-1-r21. Accessed 2022-03-23
74. Yasukochi, Y.: A Dense Genetic Map of the Silkworm, Bombyx mori, Covering All Chromosomes Based on 1018 Molecular Markers **150**(4), 1513–1525. doi:10.1093/genetics/150.4.1513. Accessed 2022-03-23
75. Jiggins, C.D., Mavarez, J., Beltrán, M., McMillan, W.O., Johnston, J.S., Bermingham, E.: A Genetic Linkage Map of the Mimetic Butterfly Heliconius melpomene **171**(2), 557–570. doi:10.1534/genetics.104.034686. 15489522. Accessed 2021-11-01
76. Tobler, A., Kapan, D., Flanagan, N.S., Gonzalez, C., Peterson, E., Jiggins, C.D., Johntson, J.S., Heckel, D.G., McMillan, W.O.: First-generation linkage map of the warningly colored butterfly Heliconius erato **94**(4), 408–417. doi:10.1038/sj.hdy.6800619. Accessed 2022-03-23
77. Kawakami, T., Mugal, C.F., Suh, A., Nater, A., Burri, R., Smeds, L., Ellegren, H.: Whole-genome patterns of linkage disequilibrium across flycatcher populations clarify the causes and consequences of fine-scale recombination rate variation in birds **26**(16), 4158–4172. doi:10.1111/mec.14197. Accessed 2020-04-30
78. Barnes, T.M., Kohara, Y., Coulson, A., Hekimi, S.: Meiotic recombination, noncoding DNA and genomic organization in Caenorhabditis elegans. **141**(1), 159–179. doi:10.1093/genetics/141.1.159. Accessed 2022-03-23
79. Scherthan, H., Weich, S., Schwegler, H., Heyting, C., Härle, M., Cremer, T.: Centromere and telomere movements during early meiotic prophase of mouse and man are associated with the onset of chromosome pairing. **134**(5), 1109–1125. doi:10.1083/jcb.134.5.1109. Accessed 2021-10-26
80. Smith, G.R., Nambiar, M.: New Solutions to Old Problems: Molecular Mechanisms of Meiotic Crossover Control **36**(5), 337–346. doi:10.1016/j.tig.2020.02.002. 32294414. Accessed 2022-03-23
81. Kent, T.V., Uzunović, J., Wright, S.I.: Coevolution between transposable elements and recombination **372**(1736), 20160458. doi:10.1098/rstb.2016.0458. Accessed 2021-09-28
82. Rizzon, C., Marais, G., Gouy, M., Biémont, C.: Recombination Rate and the Distribution of Transposable Elements in the Drosophila melanogaster Genome **12**(3), 400–407. doi:10.1101/gr.210802. 11875027. Accessed 2021-09-28
83. Deininger, P.L., Batzer, M.A.: Alu Repeats and Human Disease **67**(3), 183–193. doi:10.1006/mgme.1999.2864. Accessed 2021-09-28
84. Apuli, R.-P., Bernhardsson, C., Schiffthaler, B., Robinson, K.M., Jansson, S., Street, N.R., Ingvarsson, P.K.: Inferring the Genomic Landscape of Recombination Rate Variation in European Aspen (*Populus tremula*) **10**(1), 299–309. doi:10.1534/g3.119.400504. Accessed 2020-04-30
85. Kawakami, T., Smeds, L., Backström, N., Husby, A., Qvarnström, A., Mugal, C.F., Olason, P., Ellegren, H.: A high-density linkage map enables a second-generation collared flycatcher genome assembly and reveals the patterns of avian recombination rate variation and chromosomal evolution **23**(16), 4035–4058. doi:10.1111/mec.12810. Accessed 2020-04-30
86. Boman, J., Mugal, C.F., Backström, N.: The Effects of GC-Biased Gene Conversion on Patterns of Genetic Diversity among and across Butterfly Genomes **13**(5), 064. doi:10.1093/gbe/evab064. Accessed 2022-03-17
87. Aljanabi, S.: Universal and rapid salt-extraction of high quality genomic DNA for PCR- based techniques **25**(22), 4692–4693. doi:10.1093/nar/25.22.4692. Accessed 2021-03-06
88. Bioinformatics, B., Andrew, S.: FastQC A Quality Control Tool for High Throughput Sequence Data. `https://www.bioinformatics.babraham.ac.uk/projects/fastqc/`
89. Catchen, J., Hohenlohe, P.A., Bassham, S., Amores, A., Cresko, W.A.: Stacks: An analysis tool set for population genomics **22**(11), 3124–3140. doi:10.1111/mec.12354. Accessed 2020-04-30
90. Li, H.: Aligning sequence reads, clone sequences and assembly contigs with BWA-MEM. doi:10.48550/arXiv.1303.3997. Accessed 2022-03-23
91. Li, H., Handsaker, B., Wysoker, A., Fennell, T., Ruan, J., Homer, N., Marth, G., Abecasis, G., Durbin, R., 1000 Genome Project Data Processing Subgroup: The Sequence Alignment/Map format and SAMtools **25**(16), 2078–2079. doi:10.1093/bioinformatics/btp352. 19505943
92. Okonechnikov, K., Conesa, A., García-Alcalde, F.: Qualimap 2: Advanced multi-sample quality control for high-throughput sequencing data, 566. doi:10.1093/bioinformatics/btv566. Accessed 2021-03-06
93. Rastas, P.: Lep-MAP3: Robust linkage mapping even for low-coverage whole genome sequencing data **33**(23), 3726–3732. doi:10.1093/bioinformatics/btx494. Accessed 2020-04-30
94. Quinlan, A.R., Hall, I.M.: BEDTools: A flexible suite of utilities for comparing genomic features **26**(6), 841–842. doi:10.1093/bioinformatics/btq033. Accessed 2022-03-23
95. (2021)., R.C.T.: R: A Language and Environment for Statistical Computing. R Foundation for Statistical Computing, Vienna, Austria. `http://www.r-project.org/index.html` Accessed 2022-03-23
96. Gurevich, A., Saveliev, V., Vyahhi, N., Tesler, G.: QUAST: Quality

assessment tool for genome assemblies **29**(8), 1072–1075. doi:10.1093/bioinformatics/btt086. Accessed 2022-03-23
97. Wang, Y., Tang, H., Debarry, J.D., Tan, X., Li, J., Wang, X., Lee, T.-h., Jin, H., Marler, B., Guo, H., Kissinger, J.C., Paterson, A.H.: MCScanX: A toolkit for detection and evolutionary analysis of gene synteny and collinearity **40**(7), 49. doi:10.1093/nar/gkr1293. 22217600
98. Krzywinski, M., Schein, J., Birol, , Connors, J., Gascoyne, R., Horsman, D., Jones, S.J., Marra, M.A.: Circos: An information aesthetic for comparative genomics **19**(9), 1639–1645. doi:10.1101/gr.092759.109. Accessed 2022-03-23
99. Holt, C., Yandell, M.: MAKER2: An annotation pipeline and genome-database management tool for second-generation genome projects **12**(1), 491. doi:10.1186/1471-2105-12-491. Accessed 2022-03-23
100. Smit, A., Hubley, R., Green, P.: RepeatMasker Open-4.0. <http://www.repeatmasker.org>
101. Korf, I.: Gene finding in novel genomes **5**(1), 59. doi:10.1186/1471-2105-5-59. Accessed 2022-03-23
102. Jones, P., Binns, D., Chang, H.-Y., Fraser, M., Li, W., McAnulla, C., McWilliam, H., Maslen, J., Mitchell, A., Nuka, G., Pesseat, S., Quinn, A.F., Sangrador-Vegas, A., Scheremetjew, M., Yong, S.-Y., Lopez, R., Hunter, S.: InterProScan 5: Genome-scale protein function classification **30**(9), 1236–1240. doi:10.1093/bioinformatics/btu031. Accessed 2022-03-23
103. Bao, W., Kojima, K.K., Kohany, O.: Repbase Update, a database of repetitive elements in eukaryotic genomes **6**(1), 11. doi:10.1186/s13100-015-0041-9. Accessed 2022-03-23
104. Zhan, S., Reppert, S.M.: MonarchBase: The monarch butterfly genome database **41**(D1), 758–763. doi:10.1093/nar/gks1057. Accessed 2022-03-23
105. Huerta-Cepas, J., Szklarczyk, D., Heller, D., Hernández-Plaza, A., Forslund, S.K., Cook, H., Mende, D.R., Letunic, I., Rattei, T., Jensen, L.J., von Mering, C., Bork, P.: eggNOG 5.0: A hierarchical, functionally and phylogenetically annotated orthology resource based on 5090 organisms and 2502 viruses **47**(D1), 309–314. doi:10.1093/nar/gky1085. Accessed 2022-03-24
106. Manni, M., Berkeley, M.R., Seppey, M., Simão, F.A., Zdobnov, E.M.: BUSCO Update: Novel and Streamlined Workflows along with Broader and Deeper Phylogenetic Coverage for Scoring of Eukaryotic, Prokaryotic, and Viral Genomes **38**(10), 4647–4654. doi:10.1093/molbev/msab199. Accessed 2022-03-23
107. Emms, D.M., Kelly, S.: OrthoFinder: Phylogenetic orthology inference for comparative genomics **20**(1), 238. doi:10.1186/s13059-019-1832-y. Accessed 2021-08-24
108. Librado, P., Vieira, F.G., Rozas, J.: BadiRate: Estimating family turnover rates by likelihood-based methods **28**(2), 279–281. doi:10.1093/bioinformatics/btr623. Accessed 2021-06-15
109. Huerta-Cepas, J., Serra, F., Bork, P.: ETE 3: Reconstruction, Analysis, and Visualization of Phylogenomic Data **33**(6), 1635–1638. doi:10.1093/molbev/msw046. Accessed 2021-08-24
110. Akaike, H.: A new look at the statistical model identification **19**(6), 716–723. doi:10.1109/TAC.1974.1100705. Accessed 2022-03-23
111. Wolfe, D., Dudek, S., Ritchie, M.D., Pendergrass, S.A.: Visualizing genomic information across chromosomes with PhenoGram **6**(1), 18. doi:10.1186/1756-0381-6-18. Accessed 2022-03-23
112. Alexa, A., Rahnenfuhrer, J.: topGO: Enrichment Analysis for Gene Ontology. doi:10.18129/B9.bioc.topGO. Bioconductor version: Release (3.13). https://bioconductor.org/packages/topGO/ Accessed 2021-08-24
113. Alexa, A., Rahnenführer, J., Lengauer, T.: Improved scoring of functional groups from gene expression data by decorrelating GO graph structure **22**(13), 1600–1607. doi:10.1093/bioinformatics/btl140. Accessed 2021-08-24
114. Benjamini, Y., Hochberg, Y.: Controlling the False Discovery Rate: A Practical and Powerful Approach to Multiple Testing **57**(1), 289–300. 2346101
115. Rezvoy, C., Charif, D., Gueguen, L., Marais, G.A.B.: MareyMap: An R-based tool with graphical interface for estimating recombination rates **23**(16), 2188–2189. doi:10.1093/bioinformatics/btm315. Accessed 2021-08-24
116. Bauer, D.F.: Constructing Confidence Sets Using Rank Statistics **67**(339), 687–690. doi:10.1080/01621459.1972.10481279. Accessed 2022-03-23
117. Best, D.J., Roberts, D.E.: Algorithm AS 89: The Upper Tail Probabilities of Spearman's Rho **24**(3), 377. doi:10.2307/2347111. 2347111
118. Royston, J.P.: An Extension of Shapiro and Wilk's W Test for Normality to Large Samples **31**(2), 115. doi:10.2307/2347973. 10.2307/2347973
119. Wickham, H.: Ggplot2: Elegant Graphics for Data Analysis. Use R! Springer-Verlag. doi:10.1007/978-0-387-98141-3. https://www.springer.com/gp/book/9780387981413 Accessed 2021-08-24